

Break-up of concrete structures under internal explosion

J. Weerheijm^{#*}

[#]TNO Defence, Security and Safety, The Netherlands

^{*}Delft University of Technology Faculty of Civil Engineering and Geosciences

H.S. Lim

Defence Science and Technology Agency, Singapore

ABSTRACT: When an explosion occurs in a concrete structure, debris throw is one of the major hazards and dominates the safety distances. To gain insight into concrete break-up, a series of one-way spanning clamped concrete slabs exposed to internal blast were tested under various loading densities. A combination of special powerful X-ray pulsars, high-speed video and strain gauges are employed to capture the initial concrete deformation and its subsequent break-up process. An overview of the tests, the results and the interpretation of the break-up process are presented in this paper.

1 INTRODUCTION

The Klotz Group (KG), an international group of experts on explosion safety, has adopted a physical engineering approach in the prediction of debris hazard from internal explosion of a concrete ammunition storehouse (Weerheijm et al, 2002). In this engineering approach, the distribution of the concrete debris mass, the debris velocity and their launch angle are important parameters that affect the subsequent debris flight distance. Failure and subsequent break-up of concrete has a direct influence on all these parameters. In literature there are no experiments reported that focus on the initial response phase under explosive loading, i.e. the response phase when the concrete breaks up. In order to gain a better understanding of the break-up phenomenon, the Klotz Group is exploring the feasibility of using a combination of advanced tomographical techniques (x-ray), high speed video and strain gauges for the concrete breakup study.

2 BREAK-UP AND OVERLOADING CONDITIONS

The response and failure mode of a structure results in the final break-up and debris formation. The KG adopted the terminology of three dominant overloading conditions based on the difference in debris throw physics, i.e. the overloading conditions of composite-shock, impulsive shock and gas pressure. These conditions can be characterised as follows:

Shock overloading

Local effects happen at shock overloading at small distance of charge-to-wall. The shock load exceeds the concrete compressive strength. Spallation crater, scabbing and material failure occur. Theoretically, at high loading densities (= charge weight /internal volume) a complete wall may be destroyed in the shock-overloading mode. Typical debris size is the size of the aggregates. Scabbing debris from the structures outside starts at highest velocity, but their individual and total mass is small.

Blast impulsive overloading

The blast impulsive overloading results in minor local damage. At points of load concentration the load typically exceeds the shear strength of concrete and reinforcement steel. Typical debris size is large pieces (torn-off at weak points) or complete roof slabs torn-off along the edge restraint. Debris from blast impulse overloading starts with an initial velocity (due to direct momentum transfer) but will be accelerated to its launch velocity by the gas pressure.

Gas pressure overloading

Failure due to gas pressure overloading occurs at a much later time than in the other overloading regimes. The structure fails due to the generated gas pressure and not due to the initial shock loads. The structure distorts and the wall moves during the loading process. In some situations the structure may be blown up like a balloon. The transient load exceeds the tensile strength of concrete but not the

strength of the reinforcement steel. The concrete typically will be blown out through the reinforcement mesh. The mesh withstands and the typical debris size is the mesh size.

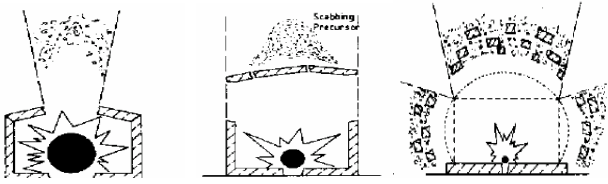


Figure 1. The three overloading regimes: shock-, blast impulsive- and gas pressure overloading, respectively.

In real life, the transition between the overloading regimes is not strict. The research reported in this paper deals with the transition from the gas pressure to the impulsive overloading regime.

3 TEST SET-UP

3.1 Explosion box

A composite steel-concrete explosion box was designed on which concrete slabs could be clamped and tested. Figure 2 shows the box and the test slabs with the dimensions. The test-slabs are designed to be representative for the case of 1/5 scale roof slabs of ammunition magazines. The average compressive cube strength at the 28th day is 46 MPa and the average tensile splitting strength is 4 MPa.

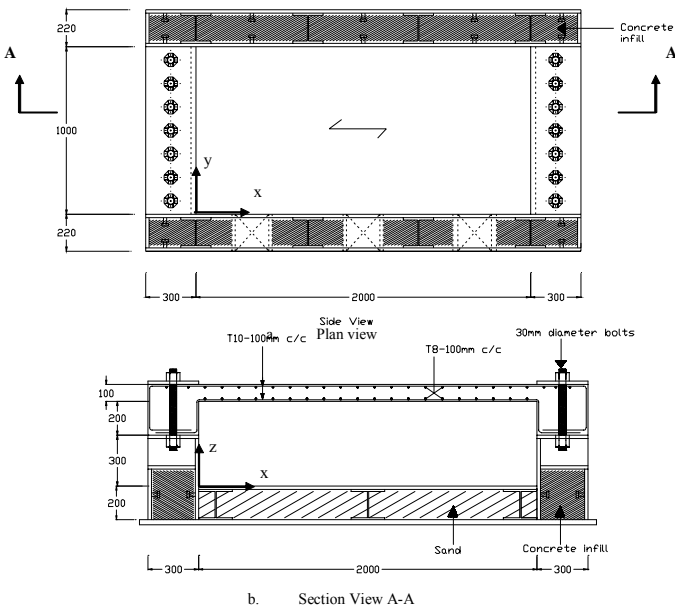


Figure 2. Explosion box with one-way clamped RC-test slab.

3.2 Test set-up

The general test layout is shown in Figure 3. There are 4 main sets of data recording: the x-rays, the high speed video, the strain gauges and the pressure history recording. There are 2 x-ray pulsars placed at

the central window shooting the side view of the slab and the 2 pulsars will produce two images at different time at different height. A high speed video is also applied to record the entire explosion event. The video is viewing from the top of the slab via a mirror. In this way, a three dimensional picture of the slab response process is recorded. The strain gauges are pasted on one half of the span to study the initial response before visible movements can be seen from the x-ray and video recordings. Three pressure transducers are placed at the sidewalls to give an indication of the load on the slab. A total of 8 tests with loading density between 0.5kg/m³ to 4 kg/m³ were conducted. The hemispherical charges are either single charge or double charges and placed at the bottom of the box.

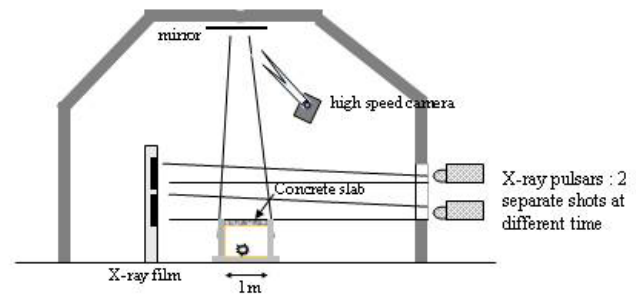


Figure 3. Experimental and diagnostic set-up.

4 TEST RESULTS

In this paper, only the head-lines of the obtained results and observations from the various diagnostic techniques are presented and discussed using the results of the 0.5 and 2 kg single charge tests. It is important to note that the diagnostic results by themselves do not provide sufficient information of the slab response nor its break-up. Hence, these results are combined and in doing so, a more consistent conclusion about the slab response and its break-up can be made.

4.1 Single charge test 0.5 kg

The information obtained from the x-ray and the high speed video are coupled to the average pressure history measured from the pressure gauges as shown in Figure 4. The slab's partial side views were taken at two heights at two different times as shown in Figure 5. Although large traverse cracks can be seen from the high speed video at t=15ms (Fig.6), the slab did not disintegrate into individual debris pieces as they are still held together by the reinforcement. The large traverse cracks are not obvious in the x-ray photos because the slab's width of 1m is too dense for the x-ray to penetrate through.

Another interesting phenomenon is that the slab continues to deform even after 16ms when the loading is almost zero. While the energy from the explo-

sion has already been transmitted to the slab by 16ms, the break-up process itself is not yet completed and a longer observation period is required. Hence, in future experiments additional x-ray shots should be taken at a much later time.

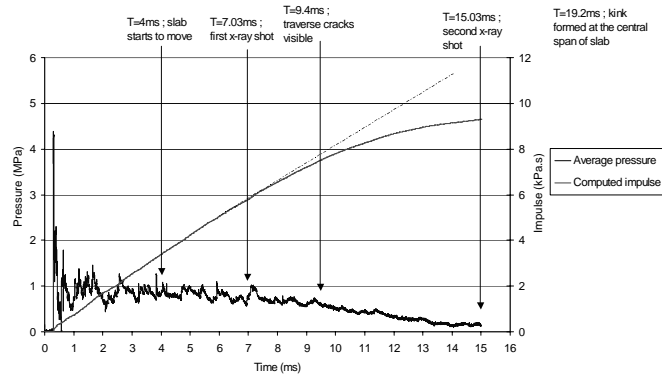


Figure 4. Pressure and impulse history for 0.5 kg test.

An attempt was made to reconstruct the slab deflection curve based on the position of the slab as given in the x-ray photos. The position of the slab outside the x-ray films are extrapolated using a simple curve fitting function in the AUTOCAD software. The result shows that the vertical displacement at the left edge is about 34mm and 73mm for $t=7.03\text{ms}$ and $t=15.03\text{ms}$ respectively. If this displacement predictions are true, then the slab will be completely sheared off by $t=15.03\text{ms}$. However, there is a possibility that the slab edge is not completely sheared off yet at $t=7.03\text{ms}$. The AUTOCAD drawings also showed a more pronounced curvature at $t=15.03\text{ms}$, suggesting that the failure is by bending.

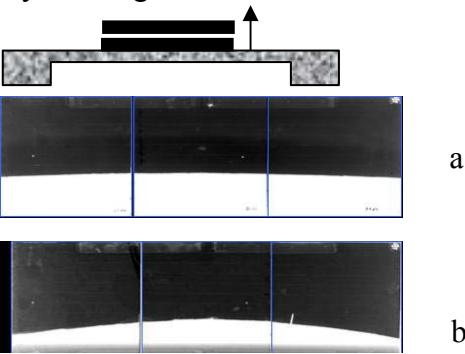


Figure 5. X-ray pictures at $t=7.03$ msec and 11.6 cm translation (a) and at $t=15.03$ msec with 38.6 cm translation.

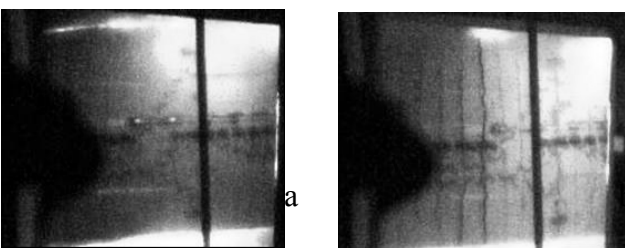


Figure 6. Snap shots from high speed recordings (a) at $t=7\text{msec}$ (no cracks visible) and (b) at $t=15$ msec with extensive lateral cracking.

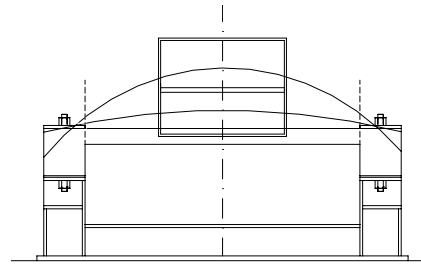


Figure 7. Extrapolated deflection curves, from X-ray shots for the 0.5 kg test.

4.2 Single charge tests 1 and 2 kg

In this section, the results of all the single charge weight tests are summarized. Obviously, the loading on the slab increases as the charge weight increases as shown in Table 1.

Table 1. Summary of the pressure recordings for singular charge tests.

Test	2	4	6	7
Charge weight (kg)	0.5	1	2	4
Peak average pressure (MPa)	4.36	6.95	7.56	26.2
Load duration (msec)	15.7	12.4	10.5	8.4
Total load impulse (kPa.s)	9.37	11.5	13.9	33.5

The x-ray photos for the 2 kg case (test 6) are shown in Figures 8. There is minimal spalling at the top of the slab and no local breaching occurs.

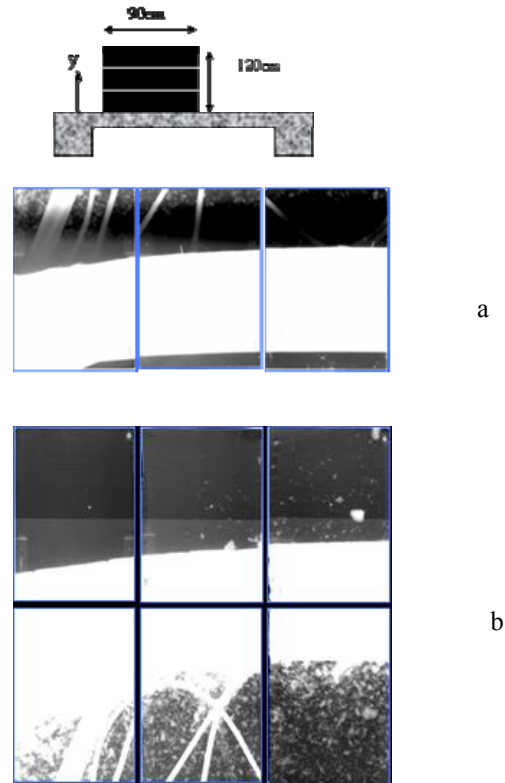


Figure 8. Side view of x-ray shots for the 2 kg test (test 6) at $t=6.37$ msec and 23.5cm translation (a) and at $t=14.33$ msec with 71.4 cm translation (b).

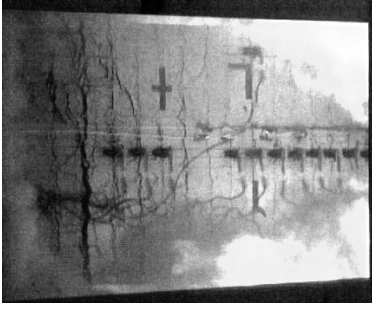


Figure 9. Snap shot high speed recording test 6, at 9.8 msec.

The second x-ray photo (Fig 8b) shows that the concrete debris is still held together by the reinforcement even though large traverse cracks can be seen from the high speed video (Fig 9). The x-ray photo also shows a lot of concrete cover spalling at the bottom of the slab. This is due to the effect of the reinforcement resistance, as the slab moves the concrete cover is pulled off. The x-ray shots from the test with 4 kg charge also show that the damaged material travels together for at least the first 50 cm.

The slabs' deflection curves based on their respective x-ray photos are reconstructed for the 2 and 4 kg tests as shown in Figure 10. (Note that the x-ray shots in the 4 kg test are taken at an earlier stage, so the travel distance is smaller than in the 2 kg test). The first x-ray shots show that the edge displacements are already more than 100mm. This implies that the slabs have already been detached from their support when the first x-ray shot is made. The high-speed video also confirms that the slabs are sheared off from its edge supports as traverse cracks can be seen at that position. Subsequently, the slab bending increases and more traverse cracks occur throughout the slab. Hence the failure mode of the slab for the 2 and 4 kg tests is shear. Further deformations in the later stages appear to be predominantly bending.

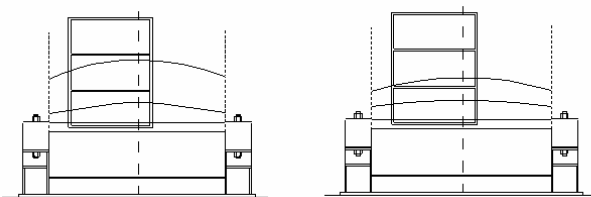


Figure 10. Extrapolated deflected shape of slab at the first and second x-ray shot for the 2kg test (left) and 4 kg test (right).

5 STRAIN MEASUREMENTS AND STRUCTURAL ANALYSIS

The test data and observations presented in the previous sections already shed some light on the failure mechanism and the role of structural response in the final failure process. In an attempt to gain information on the early time response of the structure and

especially the failure sequence, strain gauges were applied in the tests.

5.1 Strain gauge lay-out and data

The strain gauges are placed on top of the slab surface to record the deformation of the slab after the first few milliseconds of the explosion. The strain gauges are all uniaxial, measuring in the span direction. No gauges were applied in the transverse direction, assuming the dominance of one-way spanning and curvature in the traverse direction is negligible. Their positions are indicated in Figure 11. The strain gauges 1 to 10 are placed at equal distances on one side of the slab. Additional strain gauges 12 to 14 are placed to counter-check this assumption of symmetry at $x = 1000\text{mm}$. The last two gauges, 15 and 16 are placed to counter-check if curvatures near the edges are the same as curvature in the central axis ($y = 500\text{mm}$).

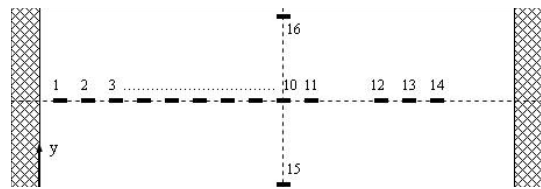


Figure 11. Position and numbering of the strain gauges on the top surface of the slabs.

Figure 12 gives an example of a set of strain gauge records. It illustrates that the recorded information is extremely complex and hard to analyse. In the early time response, the energy transfer into the slab induces stress waves. The propagating and reflecting waves lead to the (final) structural response.

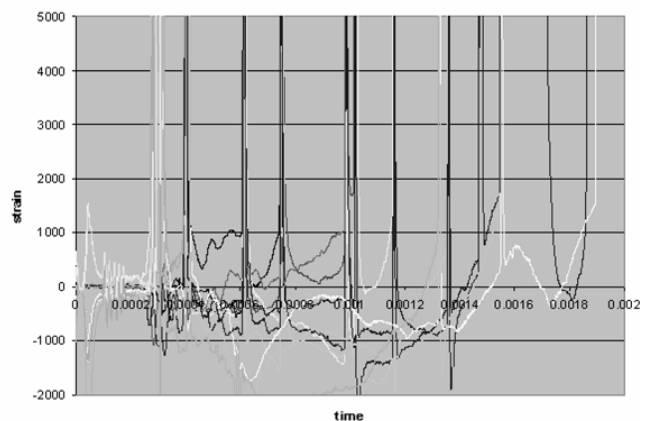


Figure 12. Example of a set of strain gauge recordings.

Therefore, the strain gauge records exhibit the (local) deformation due to the wave propagation as well as the early time structural response dominated by the higher eigenmodes of the slab. Because of the complexity and the many uncertainties, the authors decided to focus on the recorded failure sequence and combine this information with the other data and the known physical phenomena of shock loading and

structural dynamics. The failure sequence was obtained successfully from the strain records for all tests. Note that the gauges, i.e. the concrete failed in tension at strain levels between 1 – 2 ‰.

5.2 Strain gauge analysis 0.5 kg test.

To illustrate the analysis procedure, test 2 with a single charge of 0.5 kg is discussed in detail.

First the time of failure (dt_{fail}) is determined for the strain gauge locations. To analyse the local and global structural response, these times of failure were adjusted for the shock arrival times. The latter were determined using the pressure gauge data and the ConWep code (Department of the Army, 1992).

Structural response is possible after the energy is transferred to the structure by numerous stress wave rays through the slab thickness. E.g. 8 rays at a velocity of 3500 m/s through the slab of 0.1 m thickness gives that structural response is possible after 0.2 msec. Therefore, the first response just above the charge is only possible after 0.2 msec. The result (dt_{fail}) for the 0.5 kg test is given in Figure 13 and clearly shows that the slab above the charge fails immediately after the shock impact. Most probably, wave phenomena dominate and local failure occurs while the structural response is still very limited.

At the supports however, failure is delayed, structural response dominates the failure process. After the delay, a “failure wave” travels through the structure from the support towards the middle of the plate with a velocity of about 340 m/s.

- Sequence of failure starts in the centre above the charge within 0.2 – 0.4 msec, followed by the failure at the support;
- The time to failure decreases with increasing loading densities in the range of 0.5–2 kg/m³;
- For this range of loading densities, immediate failure occurs above the charge after the shock hits the slab. Then failure at the support occurs and a “bending failure wave” is initiated travelling from the support to the middle of the slab with a velocity of about 300-400 m/s;

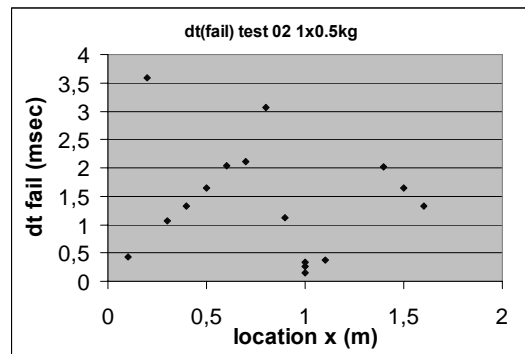
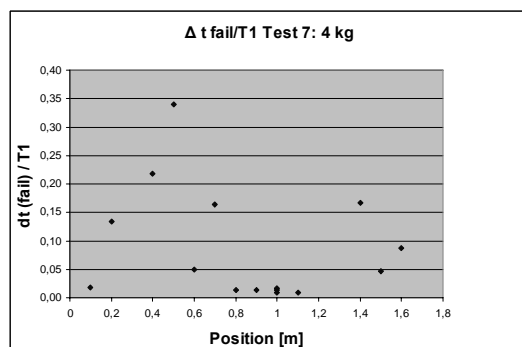
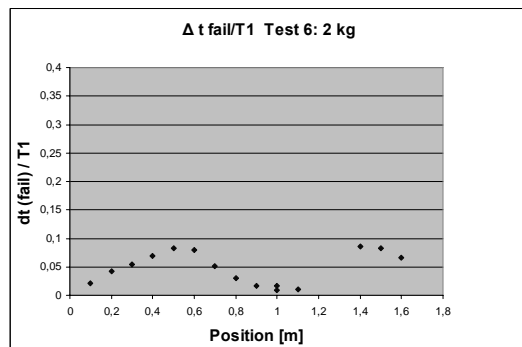
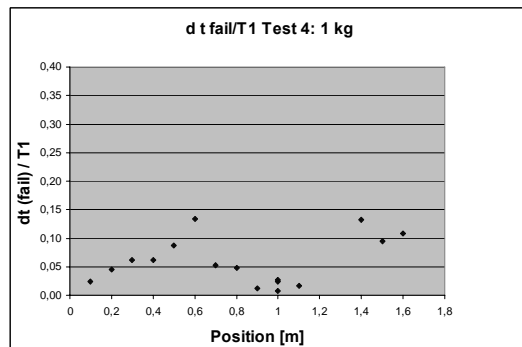
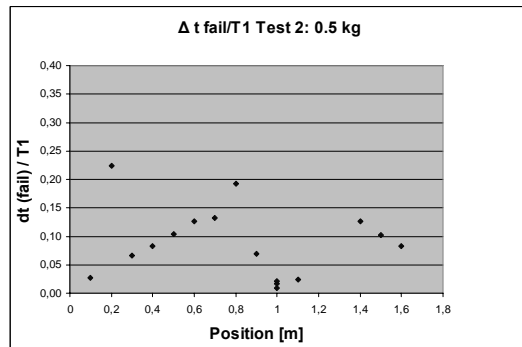


Figure 13. Time to failure dt_{fail} at strain gauge locations after shock arrival.

5.3 Strain gauge analysis for all single charge tests.

The other tests were analysed in a similar way as described for test 2. The time intervals between shock arrival and failure are given in Figure 14. Note, in this figure the intervals are related to the first eigen period of the clamped slab ($T_1 = 16.1$ msec), because the ratio t/T_1 will be used in the structural response analysis given in the next section.

The following observations are made:

Figure 14. Time interval between shock arrival and failure for the single charge tests in the 1 m³ explosion box.

- For higher loading densities, such as 4 kg/m^3 , the time to failure increases significantly, and the sequence of failure in the slab becomes less clear. From the failure sequence some “failure waves” can be recognised only for small parts of the slab and the velocities are about 300 m/s.

Conclusions:

- The failure mode changes from bending failure to shear failure at the loading density of 2 kg/m^3 .
- The strain gauge records offer the early time response information which was not provided by the optical diagnostics (high speed video and x-ray), see Figure 4.

5.4 Structural response analysis.

It is interesting to compare the test results with the mechanical response of the structure. In a theoretical study (Weerheijm et al, 2005) the dynamic response of a concrete beam/slab was studied using FE-calculations. The response was studied for LE and LE-Plastic conditions using beam-elements. In this section, only the LE-results will be used.

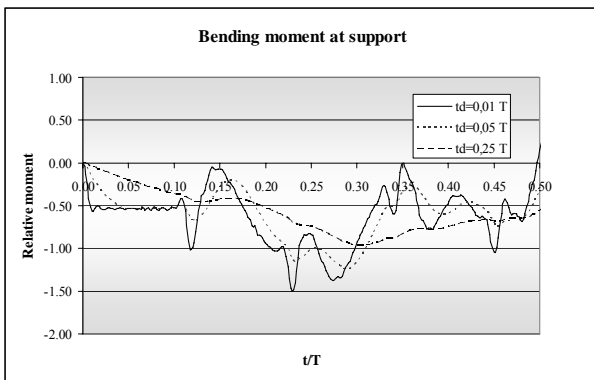


Figure 15. Bending moment at the support, related to the SDOF solution

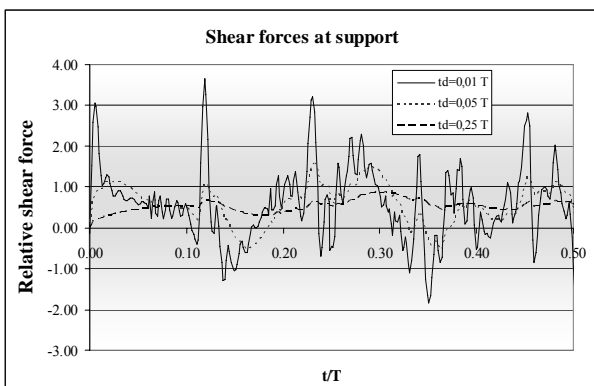


Figure 16. Shear forces at the support, related to the SDOF solution.

The shear forces and bending moments at the supports, as a function of time, are given in the Figures 15 and 16. In these figures the results are given for equally distributed loads and three load durations which are related to the first eigenperiod (T_1) of the slab i.e. 0.01 ; 0.05 and $0.25 T_1$. At the vertical axes the ratio of the “exact dynamic support reaction” and the “static support reaction times the DLF (dynamic load factor) is given. Besides the time dependency, the ratio shows the differences between the exact (FE) calculation and the simplified SDOF- approach.

To get an impression of the structural response at the time of failure, emerging from the strain gauge records, the support reactions have been compared with the static strength of the slab. The equivalent static shear force and bending moment were compared to the static bearing capacity of the slab, to get an impression to what degree the static strength has been overwhelmed in the various tests. The quantitative results are given in Table 2.

Obviously early time failure occurs due to combined bending and shear, while the shear forces are dominant. The dominance of the shear force is more pronounced with increasing charge weight. Because concrete is a highly rate dependent material, this aspect has to be taken into account. Table 3 gives the Dynamic Increase Factor (for uniaxial tension) and the adjusted ratio for the shear force at the support.

Table 2. Theoretical support reaction forces for the single charge tests for the first shock load.

Test	Peak load MPa	Dynamic / static support reaction	
		Moment	Shear
2	10	5.84	16.5
4	18	8.06	23.9
6	30	7.76	26.6
7	46	15.5	28.8

Table 3. Dynamic shear force/(resistance x DIF).

Test	Charge Kg	Load rate GPa/s	DIF	
			-	-
2	0.5	46	1.8	4
4	1	76	2.0	12
6	2	84	2.0	13
7	4	135	2.4	14

It seems that the increasing dominance of the dynamic shear forces is more or less controlled by the rate effects in concrete. Based on the LE-analysis, the increasing shear forces will not lead to a change in failure mode or mechanism. However, the contribution of the bending moment increases for small values of t_+/T_1 (Fig. 15 and Tab. 2). The combined high amplitude shear and bending might lead to

early time failure at the supports as was observed in test 7. Obviously the LE-analysis does not suffice. Advanced FE-analyses are necessary to deal with the dynamic failure process. It should be noted that due to the combined shear-bending conditions and the wave phenomena 2 and 3D-analyses are required.

Conclusion structural analysis:

- Critical location for failure of the one-way clamped plate is, evidently at the supports;
- The LE-structural analysis provides insight in force distributions and helps to interpret the tests results.
- Failure will occur due to combined shear-bending. The shear force becomes more dominant with increasing loading density. Due to the positive rate dependency of concrete, the ratio “shear force/resistance” does not change and no change in failure mode might be expected for the tested loading regimes. Note, this conclusion is based on LE-response analysis.
- For the extreme “impulsive domain” ($t_+/T_1 = 0.01$) also the bending forces increase very fast. The combined shear-bending will lead to early time shear failure. For the tested configuration, this transition might be expected at loading densities in the order of 4 kg/m^3 .
- The LE-structural response analysis did not provide clear evidence for transitions in failure mode as was observed from the strain gauge records and high speed videos. Additional research is necessary to see if the progressive failure can be explained and predicted by 2D/3D advanced FE-analysis.

Recommendation:

- Failure occurs due to combined shear-bending forces. The extreme values only occur during a very short period. Prevention of early time failure by good reinforcement design (“containment of damaged concrete”) will increase the dynamic bearing capacity of the structure significantly.

6 DEBRIS AND REINFORCEMENT

Observations of the debris and the reinforcement also provide some evidence of the response of the slab. For test 2, a large number of reinforcement grid-sized debris is found dispersed outside the steel box. Some of the reinforcement bars are not broken but are very heavily deformed as shown in Fig. 17. These evidences show that large bending deformation occurred before failure. The reinforcement played an important role in the break-up as a large number of the debris resembles the reinforcement grid size. This type of failure is classified as gas-

overpressure failure under the Klotz Group failure regime (see section on break-up modes).

For test 6 and test 7, grid-sized debris are lesser and most of the debris mass is found inside the steel box. The reinforcements failed at a shorter distance from the edge beam. These evidences show that the slab has undergone a more abrupt shear failure and the entire concrete slab translates vertically upwards. When the slab hits the roof of the bunker, it falls back into the box and that explains why most of the debris is found there. This failure mode is classified as blast-impulsive failure (see section on break-up modes).



Test 2. single charge, 0.5 kg



Test 7. single charge, 4 kg

Figure 17 Difference in reinforcement failure for 0.5 and 4 kg charge.

7 CONCLUDING REMARKS

A series of new, unique tests dedicated to study the initial stage of failure and break-up of reinforced concrete slab under explosive loading has been carried out.

The combination of x-ray photos and high-speed video show that bending failure is dominant for loading density of 0.5 kg/m^3 . For loading density beyond 2 kg/m^3 , failure is dominated by shear failure at the edge. The loading density regime of 1-2 kg/m^3 is considered as a transition between the two failure modes. Observations from the debris and re-

inforcements and also the early time response data from the strain gauges confirm these conclusions.

The LE-structural response analysis showed that failure will occur due to combined shear-bending forces. The shear force becomes more dominant with increasing loading density. Due to the strength increase of concrete at higher loading rates, the ratio “shear force/resistance” does hardly change. Based on LE-analysis, no change in failure mode might be expected for the tested loading regimes. Additional research has to be done to see if the progressive failure and observed transition in failure mode can be explained and predicted by elasto-plastic response calculations and advanced material models that represent the real dynamic concrete behaviour.

In the tests the concrete slabs do not disintegrate into individual debris during the loading phase and along the travel distance in the order of 0.5 the span-width, even though large traverse cracks are observed. This implies that a single debris velocity can be used to represent all debris during the initial break-up phase. Additional research is necessary to determine the subsequent behaviour in the break-up process.

Currently, more analysis of the data is under way. From the x-ray shots, critical information like the velocities of the slab can be determined. Numerical simulation of these experiments is planned. These analyses and results will be presented in future publications.

It is recommended to improve the experimental setup to study the full break-up process and higher loading densities. The x-ray did not capture the break-up process entirely. A more powerful x-ray pulsar and a smaller width slab will allow the fracture of the slab to be seen. Alternatively, an x-ray shot after the break-up process has been completed should also provide critical information. The tests, however, do prove that the study of concrete break-up using such advanced techniques is feasible. Critical break-up information, which was never revealed, can be obtained. The performed tests provided the first data set.

REFERENCES

- Department of the Army, *Field Manual FM 5-250 Explosives and demolition*, 15 June 1992
- Karagozian and Case, Structural Engineers, *Construction Joint Test Program (Final Report)*, Air Force Systems Command, Space and Missile Systems Organization Contract F0701-71-C-0358, Los Angeles, California, 1973.
- Lim, H.S., *Response of reinforced concrete slab to explosive loading*, MSc thesis Delft University of Technology, 2005.
- Müller, R.K., Introduction to modeling of concrete structures in *Small Scale Modelling of Concrete Structures*, (ed. F.A. Noor and L.F. Boswell), Elsevier Science Publishers Ltd. 1992, pp. 1-11.
- Nalluri, N., Featherstone, R.E., *Civil Engineering Hydraulics*, Blackwell science Ltd., 4th edition 2001.
- Pahl, P.J. & Soosaar, K., *Structural models for architectural and engineering education*. Report No. R64-3, Department of Civil Engineering, Massachusetts Institute of Technology, Cambridge, MA., 1964.
- Weerheijm, J., van Doormaal, J.C.A.M., Guerke, G. & Lim, H.S., *The breakup of ammunition magazines – Failure mechanism and debris distribution*, 30th DDESB Explosive Safety Seminar, 2002.
- Weerheijm, J.; Oldenhof, E. & Sluys, L.J., *Failure modes of reinforced concrete beams subjected to explosion loadings*, EURO-DYN conference, Paris, 2005.
- Weerheijm J., van Doormaal, J.C.A.M., *Tensile failure of concrete at high loading rates: New test data on strength and fracture energy from instrumented spalling tests*. Int. J. of Impact Engineering 34 (2007) 609-626.